
The spherical mean operator

After a short treatise about SONAR and SAR, we summarize in Section 11.2 the essential mathematical properties of the spherical mean operator \mathbf{M} . Though there are some similarities to the Radon transform \mathbf{R} with respect to its definition and inversion formula, we point out crucial differences when the center set is given by $\{x_{n+1} = 0\} \subset \mathbb{R}^{n+1}$, which causes difficulties in the numerical treatment of that mapping. The most important difference between the two transforms is the fact that \mathbf{M} can neither be formulated as continuous mapping between L^2 - nor between Sobolev spaces. Moreover, \mathbf{M} is meaningfully defined on certain spaces of tempered distributions only. Hence to solve the inverse problem

$$\mathbf{M}f = g,$$

we need the concepts presented in Chapter 4.

11.1 Spherical means in SONAR and SAR

To detect and visualize objects in the water, one emits ultrasound signals from an antenna and measures reflections. In shallow water the assumption of a constant speed of sound $c(x) = c_0$ is reasonable. A signal $U = U(t, x)$ being emitted from a source a_0 in a domain $A \subset \mathbb{R}^3$ at time $t = 0$ hence generates a spherical wave front. The reflected signal which is received at time t in a_0 thus contains information of all reflections located at a sphere with radius $(t/2)c_0$ and center a_0 , see Figure 11.1. In Figure 11.1 the center set consists of the line $\{x_2 = 0\}$.

The measured signal is

$$\mathbf{M}f(a_0, r) = \int_{S(a_0, r)} f(x) dS_n^r(x), \quad r = (t/2)c_0, \quad (11.1)$$

where $S(a_0, r) := \{x \in \mathbb{R}^3 : \|x - a_0\| = r\}$ and $f(x)$ is the reflectivity. Here dS_n^r denotes the $n-1$ -dimensional surface measure on $S(a_0, r)$. The reflectivity

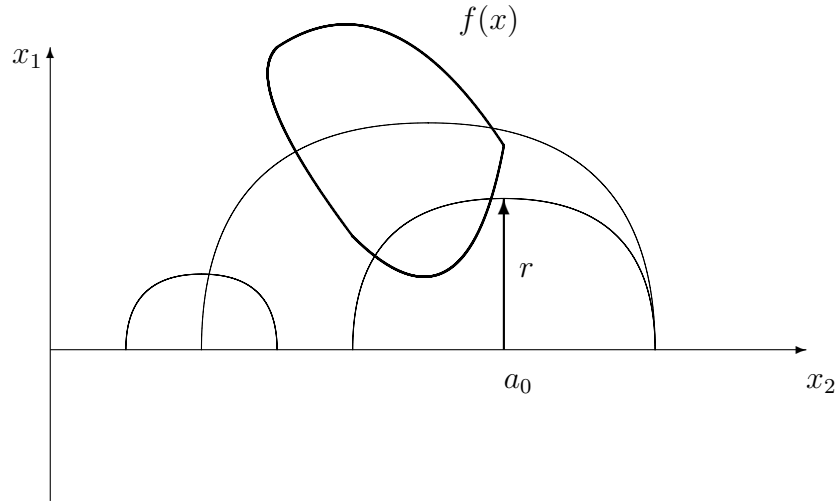


Fig. 11.1. Measurement geometry of SONAR in two dimensions. The x_1 - and x_2 -axes are switched to be consistent with the definitions in Section 11.2.

essentially depends on the speed of sound $c(x)$, which gives information about objects in the water. The problem to recover objects in water from ultrasound measurements is called SONAR (SOund NAVigation and Radiation). In SONAR the centers a_0 usually are located at the hyperplane $\{x_3 = 0\}$. As can be read in LOUIS, QUINTO [74] the signal $U(t, x)$ propagates according to the acoustic wave equation

$$k^2(x) U_{tt} = \Delta U + \delta(t) \delta(x - a_0), \quad a_0 \in A. \quad (11.2)$$

Provided that there is no multiple scattering (*Born approximation*) which means a linearization, then the determination of k^2 from the back-scattered signal is equivalent to the reconstruction of k^2 from $\mathbf{M}(k^2)(a_0, r)$, see LAVRIENTIEV ET AL. [62] and ROMANOV [104]. Here, the refraction index k^2 corresponds to the reflectivity f in (11.1).

We have a similar situation in SAR. Here, the aim is to determine objects at the earth's surface by ultrasound signals, where the antenna usually is attached to the wing of an aircraft. To be exact, we would have to consider Maxwell's equations as mathematical model. But for the sake of simplicity, one investigates equation (11.2) or the similar equation

$$U_{tt} = \Delta U + q(x) U + \delta(t) \delta(x - a_0), \quad a_0 \in A,$$

where $q(x)$ denotes the scatterer. HELLSTEN, ANDERSSON [45] show, how the measured data in SAR can be interpreted as spherical means of the ground reflectivity. CHENEY [15] explains how the signals which are measured at the antenna can be expressed by spherical means of $c^{-1}(x) - c_0^{-1}$ when we take equation (11.2) with $k^2(x) = -1/c^2(x)$ as a starting point.

11.2 Properties of the spherical mean operator

Let $\mathcal{S}(\mathbb{R}^n)$ be the space of rapidly decreasing functions in \mathbb{R}^n , i.e. the space of all functions $f \in \mathcal{C}^\infty(\mathbb{R}^n)$ for which the seminorms

$$p_m(v) = \sup_{|\alpha| \leq m} \sup_{x \in \mathbb{R}^n} (1 + \|x\|^2)^m |D^\alpha v(x)| < \infty$$

are finite for all $m \in \mathbb{N}_0$. Here, $\alpha \in \mathbb{N}_0^n$ is a multiindex and $D^\alpha := \partial_{x_1}^{\alpha_1} \cdots \partial_{x_n}^{\alpha_n}$ is the differential operator of order $|\alpha| = \alpha_1 + \cdots + \alpha_n$. The system $\{p_m\}$ induces a local convex topology which turns $\mathcal{S}(\mathbb{R}^n)$ to a *Fréchet space*. Its dual $\mathcal{S}'(\mathbb{R}^n)$ consists of all functionals which are linear and bounded on $\mathcal{S}(\mathbb{R}^n)$. That means that to each $\lambda \in \mathcal{S}'(\mathbb{R}^n)$ there exists a $m \in \mathbb{N}_0$ and a constant $C_m > 0$ satisfying

$$|\langle \lambda, v \rangle_{\mathcal{S}'(\mathbb{R}^n) \times \mathcal{S}(\mathbb{R}^n)}| \leq C_m p_m(v) \quad \text{for all } v \in \mathcal{S}(\mathbb{R}^n).$$

Thus, each $\lambda \in \mathcal{S}'(\mathbb{R}^n)$ is of finite order. The space $\mathcal{S}'(\mathbb{R}^n)$ is called the space of *tempered distributions*. The following theorem, which can be found e.g. in CONSTANTINESCU [17, Theorem 7.4], characterizes tempered distributions as (weak) derivatives of slowly increasing functions.

Theorem 11.1. *To each $\lambda \in \mathcal{S}'(\mathbb{R}^n)$ there exists a multiindex $\alpha \in \mathbb{N}_0^n$ and a continuous function P_λ of at most polynomial growth, such that*

$$\langle \lambda, v \rangle_{\mathcal{S}'(\mathbb{R}^n) \times \mathcal{S}(\mathbb{R}^n)} = (-1)^{|\alpha|} \int_{\mathbb{R}^n} P_\lambda(x) D^\alpha v(x) dx \quad (11.3)$$

for all $v \in \mathcal{S}(\mathbb{R}^n)$.

Obviously, $\mathcal{S}(\mathbb{R}^n) \subset \mathcal{S}'(\mathbb{R}^n)$ and the embedding is dense. As a consequence, the Fourier transform \mathbf{F} can be extended continuously to an isomorphism on $\mathcal{S}'(\mathbb{R}^n)$.

Following the lines in [5] we investigate the particular case where the centers a_0 in (11.1) are located on the hyperplane $\{z \in \mathbb{R}^{n+1} : z_{n+1} = 0\}$. To adapt this very situation we re-define \mathbf{M} . The spherical mean operator \mathbf{M} now particularly assigns a function $f \in \mathcal{S}(\mathbb{R}^{n+1})$ to its mean values over all spheres with radius $r \geq 0$ centered about $(z, 0)^\top \in \mathbb{R}^{n+1}$, $z \in \mathbb{R}^n$,

$$\mathbf{M}f(z, r) = \frac{1}{|S^n|} \int_{S^n} f(z + r\xi, r\eta) dS_n(\xi, \eta) = g(z, r). \quad (11.4)$$

By $|S^n|$ we denote the surface area of the n -dimensional unit sphere $S^n = \{(\xi, \eta)^\top \in \mathbb{R}^{n+1} : \xi \in \mathbb{R}^n, \eta \in \mathbb{R}, \|\xi\|^2 + \eta^2 = 1\} \in \mathbb{R}^{n+1}$, dS_n is the surface measure on S^n . In contrast to the Radon transform \mathbf{R} , the spherical mean operator integrates over n -dimensional hyperspheres S^n instead of n -dimensional planes. We often will use the notation $x = (x', x_{n+1})^\top$ for $x \in$

\mathbb{R}^{n+1} , where $x' = (x_1, \dots, x_n)^\top$ contains the first n components of x and x_{n+1} is the $(n+1)$ -st component.

Obviously, \mathbf{M} is not injective, since $\mathbf{M}f = 0$ for each $f \in \mathcal{S}(\mathbb{R}^{n+1})$ being odd with respect to the last variable. COURANT and HILBERT [18] proved that the null space of \mathbf{M} consists of all those functions which are odd in x_{n+1} . Thus, it is reasonable to restrict the domain of \mathbf{M} to the subspace $\mathcal{S}_e(\mathbb{R}^{n+1}) \subset \mathcal{S}(\mathbb{R}^{n+1})$ of all rapidly decreasing functions being even in x_{n+1} ,

$$\mathcal{S}_e(\mathbb{R}^{n+1}) := \{f \in \mathcal{S}(\mathbb{R}^{n+1}) : f(x', -x_{n+1}) = f(x', x_{n+1})\}.$$

Unfortunately, $f \in \mathcal{S}_e(\mathbb{R}^{n+1})$ does not imply that $\mathbf{M}f$ is again a rapidly decreasing function. Even worse: the image $\mathbf{M}f$ in general is neither in $L^2(\mathbb{R}^{n+1})$, nor in $L^1(\mathbb{R}^{n+1})$. This fact is emphasized in Example 11.2 in two dimensions ($n = 1$). The image of the characteristic function of two circles under \mathbf{M} , that means of a function with compact support, is not even integrable.

Example 11.2. Let $n = 1$ and $\chi_C \in L^2(\mathbb{R}^2)$ be the characteristic function of two disks which are reflected about the x_2 -axis

$$\chi_C(x) = \chi_C(x_1, x_2) = \begin{cases} 2, & \text{if } \|x - (4, 4)\| \leq 1 \text{ or } \|x - (4, -4)\| \leq 1, \\ 0, & \text{else.} \end{cases} \quad (11.5)$$

Note that χ_C is even with respect to x_2 . The picture to the left in Figure 11.2 shows a plot of χ_C for $x_2 > 0$. After some geometric considerations we compute for $z \in \mathbb{R}$ and $r > 0$

$$\mathbf{M}\chi_C(z, r) = \begin{cases} 8\pi^{-1} r \arccos\left(\frac{r^2 + d^2 - 1}{2rd}\right), & d - 1 \leq r \leq d + 1, \\ 0, & \text{else,} \end{cases}$$

where $d = \|(z, 0) - (4, 4)\|$. We integrate over spheres with radius $r > 0$; the center set is the line $\{(z, 0) : z \in \mathbb{R}\}$. The picture to the right in Figure 11.2 displays $\mathbf{M}\chi_C$ for (z, r) in $[-35, 35] \times [0, 50]$. Obviously the support of $\mathbf{M}\chi_C$ is not bounded in \mathbb{R}^2 .

This is a crucial difference compared to the Radon transform. The question arises on which spaces \mathbf{M} can be defined meaningfully as a bounded operator. To answer this question, we first introduce a subspace of $\mathcal{S}(\mathbb{R}^{2n+1})$. Let

$$\mathcal{S}_r(\mathbb{R}^n \times \mathbb{R}^{n+1}) := \{f \in \mathcal{S}(\mathbb{R}^{2n+1}) : f(z, w) = \check{f}(z, \|w\|) \text{ for } \check{f} \in \mathcal{S}_e(\mathbb{R}^{n+1})\}.$$

The space $\mathcal{S}_r(\mathbb{R}^n \times \mathbb{R}^{n+1})$ contains all functions of $\mathcal{S}(\mathbb{R}^{2n+1})$ being radially symmetric in the last $n+1$ variables. Thus we will always understand functions from $\mathcal{S}_r(\mathbb{R}^n \times \mathbb{R}^{n+1})$ as functions on $\mathbb{R}^n \times \mathbb{R}$ in virtue of the setting $f(z, r) = f(z, w)$, $r = \|w\|$. The reason to use \mathbb{R}^{n+1} for the radial variable rather than \mathbb{R} is that we may apply the Fourier transform to a function from $\mathcal{S}_r(\mathbb{R}^n \times \mathbb{R}^{n+1})$. This is important in view of Theorem 11.3. Of course the Fourier transform again is radial in the last $n+1$ variables. In analogy to $(\mathcal{S}(\mathbb{R}^n), \mathcal{S}'(\mathbb{R}^n))$ we may

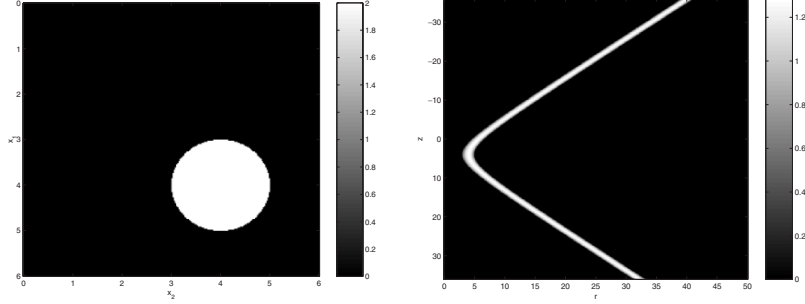


Fig. 11.2. Left picture: Plot of the object function χ_C consisting of two disks reflected about the x_2 -axis. Only the part for $x_2 > 0$ is shown. Right picture: Plot of $\mathbf{M}\chi_C$ in $[-35, 35] \times [0, 50]$.

also consider the dual pairings $(\mathcal{S}_e(\mathbb{R}^{n+1}), \mathcal{S}'_e(\mathbb{R}^{n+1}))$, $(\mathcal{S}_r(\mathbb{R}^n \times \mathbb{R}^{n+1}), \mathcal{S}'_r(\mathbb{R}^n \times \mathbb{R}^{n+1}))$. For the sake of a better readability, we set $\mathcal{S}_e := \mathcal{S}_e(\mathbb{R}^{n+1})$ and $\mathcal{S}_r := \mathcal{S}_r(\mathbb{R}^n \times \mathbb{R}^{n+1})$, the notations \mathcal{S}'_e , \mathcal{S}'_r are respectively. As a consequence of the considerations made before, we cannot expect that $\mathbf{M}f \in \mathcal{S}_r$, when $f \in \mathcal{S}_e$. But it is easy to show that $\mathbf{M}f \in \mathcal{S}'_r$ for all $f \in \mathcal{S}_e$. Since $\mathcal{S}_e \hookrightarrow \mathcal{S}'_e$ is dense, we even have $\mathbf{M}f \in \mathcal{S}'_r$ whenever $f \in \mathcal{S}'_e$. Further properties are summarized in the following theorem whose proof can be found in ANDERSSON [5] and KLEIN [59].

Theorem 11.3. *The spherical mean operator $\mathbf{M} : \mathcal{S}'_e \rightarrow \mathcal{S}'_r$ is a linear, continuous mapping which is one-to-one. The range $\mathbf{R}(\mathbf{M})$ can be characterized by*

$$\mathbf{R}(\mathbf{M}) = \mathcal{S}'_{r, \text{cone}} := \left\{ g \in \mathcal{S}'_r : \text{supp } \hat{g} \subset \{(\sigma, \varrho) \in \mathbb{R}^n \times [0, \infty) : \varrho \geq \|\sigma\|\} \right\} \subset \mathcal{S}'_r. \quad (11.6)$$

If the Fourier transform of $f \in \mathcal{S}'_e$ is equal to an integrable function $\hat{f}(\sigma, \varrho)$, then the inversion formula

$$\hat{f}(\sigma, \varrho) = c_n |\varrho| (\|\sigma\|^2 + \varrho^2)^{(n-1)/2} \hat{g}(\sigma, \sqrt{\|\sigma\|^2 + \varrho^2}) \quad (11.7)$$

holds true with $c_n = |S^n|/(2(2\pi)^n)$ and $g = \mathbf{M}f$.

The adjoint operator $\mathbf{M}^* : \mathcal{S}_r \rightarrow \mathcal{S}_e$ has dense range and is given by

$$\mathbf{M}^*g(x', x_{n+1}) = \int_{\mathbb{R}^n} g\left(z, \sqrt{\|z - x'\|^2 + x_{n+1}^2}\right) dz. \quad (11.8)$$

We further have

$$\mathbf{F} \mathbf{M}^*g(\sigma, \varrho) = \hat{g}(\sigma, \sqrt{\|\sigma\|^2 + \varrho^2}). \quad (11.9)$$

Note that the function \hat{g} on the right-hand side of equation (11.7) is a Fourier transform of a function on \mathbb{R}^{2n+1} , which is radially symmetric with respect to the last $n+1$ variables, and so is \hat{g} . In the entire Part III, we

define the Fourier transform *without* the normalizing factor $(2\pi)^{-n/2}$ to be consistent with ANDERSSON's article [5].

Remark 11.4. The adjoint operator \mathbf{M}^* integrates a function $g \in \mathcal{S}_r$ over all spheres containing the point $x = (x', x_{n+1})^\top$. That is why \mathbf{M}^* is called *back-projection* just as in case of the Radon transform \mathbf{R} . But in contrast to \mathbf{R}^* , the adjoint \mathbf{M}^* maps rapidly decreasing functions to rapidly decreasing functions.

We further remark that it is not possible to formulate the spherical mean operator as linear, bounded mapping between Sobolev spaces of negative order. This becomes clear by Figure 11.2 showing that a function, which is not continuous, has a range of large local smoothness or by the estimate

$$\|f\|_{H^\alpha(\mathbb{R}^{n+1})} \leq \sqrt{\frac{|S^n|}{2}} \|\mathbf{M}f\|_{H^{\alpha+1/2}(\mathbb{R}^{2n+1})} \quad (11.10)$$

and its proof which can be read in [5, Theorem 3.1]. Note that the Sobolev norm at the right-hand side of the estimate does not need to be finite.

Defining the operator $\mathbf{K} : H^\alpha(\mathbb{R}^{n+1}) \cap \mathcal{S}'_{r,cone} \rightarrow H^{\alpha+n}(\mathbb{R}^{2n+1}) \cap \mathcal{S}'_r$ via $\mathbf{K}g(\sigma, \varrho) = \sqrt{\varrho^2 - \|\sigma\|^2} \varrho^{n-1} \hat{g}(\sigma, \varrho)$, the inversion formula (11.7) has the representation

$$f = c_n \mathbf{M}^* \mathbf{K} \mathbf{M} f$$

and hence a structure which is according to the inversion formula (2.19) of \mathbf{R} .

We aim to transfer the concepts of Chapter 4 to the problem of solving

$$\mathbf{M}f = g. \quad (11.11)$$

To compute reconstruction kernels, we need a solution of

$$\mathbf{M}^* v_\gamma(y) = e_\gamma(y), \quad e_\gamma(y) \in \mathcal{S}_e. \quad (11.12)$$

Theorem 11.3 tells us that we have the situation described in part b) of Remark 4.3: if $e_\gamma(y) \in \mathbf{R}(\mathbf{M}^*)$, then $v_\gamma(y)$ lies in \mathcal{S}_r . Against this background, the extension lemma [5, Lemma 2.4] is of great importance.

Lemma 11.5. *There exists a linear and continuous mapping $\mathbf{E} : \mathcal{S}_e \rightarrow \mathcal{S}_r$ satisfying*

$$\mathbf{M}^* \mathbf{E} = 1_{\mathcal{S}_e}, \quad (11.13)$$

where $1_{\mathcal{S}_e}$ denotes the identity on \mathcal{S}_e , $1_{\mathcal{S}_e}(f) = f$, $f \in \mathcal{S}_e$. For $\varrho \geq \|\sigma\|$ the mapping \mathbf{E} is characterized by the Fourier transform

$$\mathbf{E}f(\sigma, \varrho) = \hat{f}(\sigma, \sqrt{\varrho^2 - \|\sigma\|^2}), \quad \sigma \in \mathbb{R}^n, \varrho \geq 0. \quad (11.14)$$

Identity (11.13) can easily be deduced from (11.14) with the help of representation (11.9). The crucial difficulty of proving Lemma 11.5 is to extend

FE for $\rho < \|\sigma\|$. ANDERSSON uses in [5] an extension theorem contained in the book of STEIN [123]. Since this theorem does not provide an explicit representation of **FE**, we will use another technique to obtain an extension in Chapter 12.

To increase the efficiency of the inversion method, we used the existence of invariances in case of an operator between Hilbert spaces. Lemma 4.5 promises an improvement in efficiency in the distributional case, too, as long as an intertwining property applies to the adjoint \mathbf{M}^* , since \mathbf{M} is one-to-one on \mathcal{S}'_e . Lemma 11.6 will show that such an intertwining in fact does exist. But first, we introduce some notations.

For real $M > 1$ we distinguish certain open subsets of \mathbb{R}^{n+1} . We define

$$\begin{aligned}\mathcal{H}^M &:= \mathcal{H}^M(\mathbb{R}^{n+1}) = \{y = (y', y_{n+1})^\top \in \mathbb{R}^{n+1} : 1/M < |y_{n+1}|\}, \\ \mathcal{H}^{M,M} &:= \mathcal{H}^{M,M}(\mathbb{R}^{n+1}) = \{y = (y', y_{n+1})^\top \in \mathbb{R}^{n+1} : 1/M < |y_{n+1}| < M\}.\end{aligned}$$

Since the invariances in (11.15), (11.16) use dilations in y_{n+1} , the reconstruction points y must be contained in the complement of the hyperplane $y_{n+1} = 0$. That is why we introduced the set \mathcal{H}^M . To state convergence results as in Corollary 11.7 we even have to postulate that y_{n+1} is bounded. That is the reason to define $\mathcal{H}^{M,M}$. For an open subset $U \subset \mathbb{R}^{n+1}$ we denote

$$\begin{aligned}\mathcal{S}_e(U) &:= \{v \in \mathcal{S}_e : \text{supp } v \subset U\}, \\ \mathcal{S}'_e(U) &:= \{\lambda \in \mathcal{S}'_e : \text{supp } \lambda \subset U\}, \\ \mathcal{E}'_e(U) &:= \{\lambda \in \mathcal{S}'_e : \text{supp } \lambda \subset U \text{ is compact}\}.\end{aligned}$$

Note that in general $\mathcal{S}'_e(U)$ represents a proper subspace of $\mathcal{S}_e(U)'$. Finally, let mappings $\mathcal{T}_{e,M}^y : \mathcal{S}_e \rightarrow \mathcal{S}_e$ and $\mathcal{G}_{r,M}^y : \mathcal{S}_r \rightarrow \mathcal{S}_r$ be defined by

$$\mathcal{T}_{e,M}^y v(x) = \begin{cases} |y_{n+1}|^{-n-1} v\left(\frac{x'-y'}{|y_{n+1}|}, \frac{x_{n+1}}{|y_{n+1}|}\right), & y \in \mathcal{H}^M(\mathbb{R}^{n+1}), \\ 0, & y \notin \mathcal{H}^M(\mathbb{R}^{n+1}), \end{cases} \quad (11.15)$$

$$\mathcal{G}_{r,M}^y w(z, r) = \begin{cases} |y_{n+1}|^{-2n-1} w\left(\frac{z-y'}{|y_{n+1}|}, \frac{r}{|y_{n+1}|}\right), & y \in \mathcal{H}^M(\mathbb{R}^{n+1}), \\ 0, & y \notin \mathcal{H}^M(\mathbb{R}^{n+1}). \end{cases} \quad (11.16)$$

Obviously, $\mathcal{T}_{e,M}^y$ and $\mathcal{G}_{r,M}^y$ are linear and bounded as compositions of translations and dilations. But nevertheless $\mathcal{T}_{e,M}^y v$ as well as $\mathcal{G}_{r,M}^y w$ may be discontinuous in y for $y_{n+1} = \pm 1/M$. Both mappings fulfill the desired intertwining property with respect to \mathbf{M}^* .

Lemma 11.6. *Let $\mathcal{T}_{e,M}^y : \mathcal{S}_e \rightarrow \mathcal{S}_e$ and $\mathcal{G}_{r,M}^y : \mathcal{S}_r \rightarrow \mathcal{S}_r$ be given as in (11.15), (11.16) respectively. Then*

$$\mathcal{T}_{e,M}^y \mathbf{M}^* = \mathbf{M}^* \mathcal{G}_{r,M}^y, \quad y \in \mathbb{R}^{n+1}. \quad (11.17)$$

Proof. When $y \notin \mathcal{H}^M(\mathbb{R}^{n+1})$, then there is nothing to show, since both sides of (11.17) are equal to zero.

Let $y \in \mathcal{H}^M(\mathbb{R}^{n+1})$. Using representation (11.8) and appropriate substitutions yield

$$\begin{aligned}
\mathbf{M}^* \mathcal{G}_{r,M}^y w(x', x_{n+1}) &= \\
&= |y_{n+1}|^{-2n-1} \int_{\mathbb{R}^n} w\left(\frac{z-y'}{|y_{n+1}|}, |y_{n+1}|^{-1} \sqrt{\|z-x'\|^2 + x_{n+1}^2}\right) dz \\
&= |y_{n+1}|^{-n-1} \int_{\mathbb{R}^n} w\left(z - |y_{n+1}|^{-1} y', \sqrt{\|z - |y_{n+1}|^{-1} x'\|^2 + |y_{n+1}|^{-2} x_{n+1}^2}\right) dz \\
&= |y_{n+1}|^{-n-1} \int_{\mathbb{R}^n} w\left(z, \sqrt{\|z - |y_{n+1}|^{-1} (x' - y')\|^2 + |y_{n+1}|^{-2} x_{n+1}^2}\right) dz \\
&= \mathcal{T}_{e,M}^y \mathbf{M}^* w(x', x_{n+1}),
\end{aligned}$$

where $w \in \mathcal{S}_r$. This completes the proof. \square

Lemma 11.6 allows for solving equation (11.12) for a *single* $y \in \mathbb{R}^{n+1}$ only.

We conclude this section by remarking that the transform $\mathcal{T}_{e,\infty}^y := \lim_{M \rightarrow \infty} \mathcal{T}_{e,M}^y$ is a representation of the group $(\mathbb{R}^n, +) \times ((0, +\infty), \cdot)$. The identity element of that group is $(0, \dots, 0, 1)^\top$ which is exactly that point for which equation (11.12) is to be solved. Thus, the invariances are adjusted to the given measurement geometry.

11.3 Approximate inverse for M

We give an outline how to transfer the abstract framework of distributional approximate inverse from Chapter 4 to the spherical mean operator \mathbf{M} . We identify $\mathbf{A} = \mathbf{M}$, $V = \mathcal{S}_e$, $W = \mathcal{S}_r$, $\mathcal{T}_1^y = \mathcal{T}_{e,M}^y$ and $\mathcal{T}_2^y = \mathcal{G}_{r,M}^y$ and consider first the continuous problem (11.11). At the end of this section, we briefly deal with the semi-discrete setting which is necessary for the implementation of the method in Chapter 14.

Assume that we have an $e_\gamma(y)$ at hand which is in \mathcal{S}_e for every $y \in \mathbb{R}^{n+1}$ and satisfies the requirements to be a mollifier according to Definition 4.1. The reconstruction kernel $v_\gamma(y)$ associated with $e_\gamma(y)$ solves equation (11.12) and is an element of \mathcal{S}_r for every $y \in \mathbb{R}^{n+1}$ due to part b) from Remark 4.3 and Theorem 11.3. Applying Lemma 11.5, we immediately see that

$$v_\gamma(y) = \mathbf{E}e_\gamma(y) \quad (11.18)$$

fulfills (11.12). The intertwining property (11.17) enables us to solve equation (11.18) for $y = (0, \dots, 0, 1) \in \mathbb{R}^{n+1}$ only.

Corollary 11.7. *For all $\gamma > 0$ let $\bar{e}_\gamma \in \mathcal{S}_e(\mathbb{R}^{n+1})$ and $e_\gamma(y) \in \mathcal{S}_e(\mathbb{R}^{n+1})$ be generated for fixed $M > 1$ by the transform $\mathcal{T}_{e,M}^y$,*

$$e_\gamma(y) = \mathcal{T}_{e,M}^y \bar{e}_\gamma, \quad y \in \mathbb{R}^{n+1}. \quad (11.19)$$

Assume that e_γ is a mollifier for \mathbf{M} according to Definition 4.1. Then all corresponding reconstruction kernels $v_\gamma(y)$ are obtained by

$$\bar{v}_\gamma = \mathbf{E}\bar{e}_\gamma \quad (11.20)$$

and

$$v_\gamma(y) = v_\gamma(y)(z, r) = \mathcal{G}_{r, M}^y \bar{v}_\gamma(z, r). \quad (11.21)$$

If e_γ is a $(\mathcal{E}'_e(\mathcal{H}^{M, M}), \mathcal{S}_e(\mathcal{H}^{M, M}))$ -mollifier according to Definition 4.1, then

$$\widetilde{\mathbf{M}}_\gamma \mathbf{M}f := \langle \mathbf{M}f, v_\gamma(\cdot) \rangle_{\mathcal{S}'_t \times \mathcal{S}_r} \rightarrow f \quad \text{as } \gamma \rightarrow 0$$

for all $f \in \mathcal{E}'_e(\mathcal{H}^{M, M})$. That means

$$\lim_{\gamma \rightarrow 0} \langle \langle \mathbf{M}f, v_\gamma(\cdot) \rangle_{\mathcal{S}'_t \times \mathcal{S}_r}, \beta \rangle_{\mathcal{E}'_e(\mathcal{H}^{M, M}) \times \mathcal{S}_e(\mathcal{H}^{M, M})} = \langle f, \beta \rangle_{\mathcal{E}'_e(\mathcal{H}^{M, M}) \times \mathcal{S}_e(\mathcal{H}^{M, M})}$$

whenever $\beta \in \mathcal{S}_e(\mathcal{H}^{M, M})$.

Proof. Obviously, $\bar{v} = \mathbf{E}\bar{e}_\gamma$ satisfies $\mathbf{M}^* \bar{v} = \bar{e}_\gamma$. Lemma 11.6 then gives the identities

$$e_\gamma(x, y) = \mathcal{T}_{e, M}^y \bar{e}_\gamma(x) = \mathcal{T}_{e, M}^y \mathbf{M}^* \bar{v}_\gamma = \mathbf{M}^* \mathcal{G}_{r, M}^y \bar{v}_\gamma(x) = \mathbf{M}^* \{v_\gamma(y)\}(x).$$

Taking into account that $\mathbf{M}^* v_\gamma(y) = e_\gamma(y)$, the convergences are conclusions from Definition 4.1. \square

Remark 11.8. The fact that $e_\gamma(y)$ is generated by $\mathcal{T}_{e, M}^y$ implies that

$$\text{supp } \widetilde{\mathbf{M}}_\gamma \mathbf{M}f \subset \mathcal{H}^M.$$

As a consequence we can only recover objects $f(y)$ whose support has a distance greater than $1/M$ from the plane $\{y_{n+1} = 0\}$. This is not a restriction for applications in SONAR and SAR, since the objects to be detected always have a positive distance from the measure plane $\{y_{n+1} = 0\}$. Thus, the objects always are supported in $\mathcal{H}^M(\mathbb{R}^{n+1})$ for sufficiently large M .

We will present a criterion for \bar{e}_γ which guarantees that (11.19) generates a $(\mathcal{E}'_e(\mathcal{H}^{M, M}), \mathcal{S}_e(\mathcal{H}^{M, M}))$ -mollifier in Chapter 12. Essentially, it is sufficient for \bar{e}_γ to have mean value 1. Note that Corollary 11.7 says that using a $(\mathcal{E}'_e(\mathcal{H}^{M, M}), \mathcal{S}_e(\mathcal{H}^{M, M}))$ -mollifier we have (weak) convergence of $\widetilde{\mathbf{M}}_\gamma \mathbf{M}f$ for distributions f with support in $\mathcal{H}^{M, M}(\mathbb{R}^{n+1})$ only. But again, M may be arbitrarily large.

Besides the translation invariance \mathbf{M} has a dilation invariance, too. We have

$$\mathbf{M}^* \mathcal{D}^\gamma g(x) = \gamma^{-n-1} \mathbf{M}^* g(\gamma^{-1} x)$$

with $\mathcal{D}^\gamma g(z, r) = \gamma^{-2n-1} g(z/\gamma, r/\gamma)$. Thus, it would preferable to transfer this property to the mollifier $e_\gamma(y)$ by $e_\gamma(x, y) := \gamma^{-n-1} \mathcal{T}_{e, M}^y \bar{e}_1(x/\gamma)$. But unfortunately, such an e_γ does not fulfill the mollifier property of Definition 4.1 anymore.

We summarize the method of approximate inverse for solving $\mathbf{M}f = g$, $f \in \mathcal{E}'_e(\mathcal{H}^{M,M})$.

- Choose $\bar{e}_\gamma \in \mathcal{S}_e(\mathbb{R}^{n+1})$ such that

$$e_\gamma(x, y) = \mathcal{T}_{e,M}^y \bar{e}_\gamma(x)$$

is a mollifier.

- Compute $\bar{v}_\gamma = \mathbf{E}\bar{e}_\gamma$.
- Evaluate

$$\widetilde{\mathbf{M}}_\gamma g(y) = \langle g, \mathcal{G}_{r,M}^y \bar{v}_\gamma \rangle_{\mathcal{S}'_r \times \mathcal{S}_r} \quad (11.22)$$

for $y \in \mathcal{H}^{M,M}(\mathbb{R}^{n+1})$.

The crucial task in applying this algorithm is the computation of $\bar{v}_\gamma = \mathbf{E}\bar{e}_\gamma$. Representation (11.14) of $\mathbf{F}\mathbf{E}g$ is valid only for $\varrho \geq \|\sigma\|$. To calculate \bar{v}_γ , we need $\mathbf{F}\mathbf{E}\bar{e}_\gamma$ for all $\varrho \geq 0$. This fact has to be taken into account when designing an appropriate mollifier.

Remark 11.9. By means of Parseval's identity $\widetilde{\mathbf{M}}_\gamma g$ can be expressed by

$$\widetilde{\mathbf{M}}_\gamma g(y) = (2\pi)^{-2n-1} \langle \mathbf{F}g, \mathbf{F}\mathcal{G}_{r,M}^y \bar{v}_\gamma \rangle_{\mathcal{S}'_r \times \mathcal{S}_r}.$$

From (11.6) we see that

$$\text{supp } \mathbf{F}g = \text{supp } \mathbf{F}\mathbf{M}f \subset \{(\sigma, \varrho) \in \mathbb{R}^n \times [0, \infty) : \varrho \geq \|\sigma\|\}.$$

Hence, it seems sufficient to have knowledge of \bar{v}_γ for $\varrho \geq \|\sigma\|$ only. But then it would be necessary to calculate the Fourier transform of the measured data, which ought to be avoided for two reasons. A discrete Fourier transform would extend the data periodically, which are known in a bounded domain only, leading to artifacts. On the other hand, we would have to calculate a three-dimensional Fourier transform in the 2D case ($n = 1$) and a Fourier transform in five dimensions for the 3D case ($n = 2$) which would decrease efficiency of the method significantly, since we could not use the radial symmetry in the last $n + 1$ variables of $\mathbf{M}f$.

We conclude the chapter by dealing with the semi-discrete setting which is of great importance from a practical point of view. To this end, let $f \in \mathcal{E}'_e(\mathcal{H}^{M,M})$ be such that $\mathbf{M}f$ can be identified with a continuous function which does not need to be integrable. If the measured data $\mathbf{M}f$ are given for $p + 1$ centers $z_k \in \mathbb{R}^n$, $k = 0, \dots, p$ and for $q + 1$ radii r_l , $r_0 < r_1 < \dots < r_q$, then we have to solve

$$\Psi_N \mathbf{M}f = g_N, \quad g_N \in \mathbb{R}^N, \quad N = (p + 1)(q + 1). \quad (11.23)$$

The observation operator $\Psi_N : \mathcal{C}(\mathbb{R}^n \times \mathbb{R}_0^+) \rightarrow \mathbb{R}^N$ is defined by

$$(\Psi_N w)_{k,l} = w(z_k, r_l), \quad k = 0, \dots, p, \quad l = 0, \dots, q.$$

As we do not have a rigorous convergence theory as in the case of Hilbert spaces, we have to define the semi-discrete approximate inverse in another way. Since we have only a finite number of data and $\mathbf{M}f$ is a continuous function, the dual pairing on the right-hand side of (11.22) is a double integral with a bounded domain of integration. This suggests the application of numerical integration leading to

$$\widetilde{\mathbf{M}}_{N,\gamma} g_N(y) := \langle g_N, \mathcal{Q}_N \Psi_N \mathcal{G}_{r,M}^y \bar{v}_\gamma \rangle_{\mathbb{R}^N}. \quad (11.24)$$

The weights from numerical integration are contained in the matrix $\mathcal{Q}_N \in \mathbb{R}^{N \times N}$. The continuity of $\mathbf{M}f(z, r) \mathcal{G}_{r,M}^y \bar{v}_\gamma(z, r)$ yields pointwise convergence

$$\lim_{N \rightarrow \infty} \widetilde{\mathbf{M}}_{N,\gamma} \Psi_N \mathbf{M}f(y) = \langle \mathbf{M}f, \mathcal{G}_{r,M}^y \bar{v}_\gamma \rangle_{L^2(\text{ch}_\infty \times [0, r_\infty])}, \quad (11.25)$$

where ch_∞ and r_∞ are defined via

$$\text{ch}_\infty := \bigcup_{p=1}^{\infty} \text{ch}(\{z_k\}_{k=0}^p), \quad r_\infty := \lim_{q \rightarrow \infty} r_q$$

and $\text{ch}(\{z_k\})$ denotes the convex hull of the centers $\{z_k\}$, $k = 0, \dots, p$, in \mathbb{R}^n . The right-hand side of (11.25) equals $\langle f, e_\gamma(y) \rangle_{\mathcal{S}'_e \times \mathcal{S}_e}$, if $\text{ch}_\infty = \mathbb{R}^n$ and $r_\infty = +\infty$. For $\gamma \rightarrow 0$, we obtain then (weak) convergence to f .

It is an open question, whether this is possible or not, and how the three parameters $\gamma \rightarrow 0, p, q \rightarrow \infty$ must be coupled to get convergence as in Corollary 8.4.